

LBNL-41133
 UCB-PTH-97/60
 hep-ph/9712499
 December 1997

Tevatron Signatures of Long-lived Charged Sleptons in Gauge-Mediated Supersymmetry Breaking Models *

Jonathan L. Feng and Takeo Moroi

*Theoretical Physics Group
 Ernest Orlando Lawrence Berkeley National Laboratory
 and
 Department of Physics
 University of California, Berkeley, California 94720*

Abstract

In supersymmetric models with gauge-mediated supersymmetry breaking, charged sleptons are the next lightest supersymmetric particles and decay outside the detector for large regions of parameter space. In such scenarios, supersymmetry may be discovered by searches for a number of novel signals, including highly ionizing tracks from long-lived slow charged particles and excesses of multi-lepton signals. We consider this scenario in detail and find that the currently available Tevatron data probes regions of parameter space beyond the kinematic reach of LEP II. Future Tevatron runs with integrated luminosities of 2, 10, and 30 fb^{-1} probe right-handed slepton masses of 110, 180, and 230 GeV and Wino masses of 310, 370, and 420 GeV, respectively, greatly extending current search limits.

12.60.Jv, 14.80.Ly, 14.60.Hi, 11.30.Pb

Typeset using REVTeX

*This work was supported in part by the Director, Office of Energy Research, Office of High Energy and Nuclear Physics, Division of High Energy Physics of the U.S. Department of Energy under Contract DE-AC03-76SF00098, and in part by the National Science Foundation under grant PHY-95-14797.

I. INTRODUCTION

Supersymmetry (SUSY) provides an interesting framework for stabilizing the electroweak scale against radiative corrections. A realistic realization of this idea is the minimal supersymmetric standard model (MSSM), the model with minimal field content in which all the standard model particles have their superpartners. In the MSSM, however, the mechanism for SUSY breaking is not specified, but is simply parametrized by introducing a large number of soft SUSY breaking parameters by hand. The MSSM is therefore best viewed as the low energy effective theory of some more fundamental theory, which must give a phenomenologically viable explanation of the origin of SUSY breaking.

Models with gauge-mediated SUSY breaking [1,2] are candidates for such a theory, and provide an appealing way to generate SUSY breaking soft terms in the MSSM Lagrangian. In these models, SUSY breaking originates in a dynamical SUSY breaking sector and is then mediated via gauge interactions to the MSSM sector. The SUSY breaking mechanism does not distinguish between flavors, and so, in the MSSM sector, all scalars with identical gauge quantum numbers have the same SUSY breaking mass (at the scale where the SUSY breaking fields are integrated out). Thus, the universality of squark and slepton masses at some scale is guaranteed, and serious SUSY flavor-changing neutral current (FCNC) problems can be evaded.

To preserve the natural suppression of FCNCs in gauge-mediated SUSY breaking models, it is essential that no large intergenerational scalar mixing terms be introduced by supergravity contributions. In the absence of assumptions concerning the flavor structure of such supergravity contributions, these mixing terms are expected to be of order the gravitino mass $m_{3/2} \sim F_{\text{DSB}}/M_P$, where $F_{\text{DSB}}^{1/2}$ is the scale of dynamical supersymmetry breaking, and M_P is the Planck mass. FCNC constraints then require $m_{3/2} \ll m_W$. The gravitino is therefore the lightest supersymmetric particle,¹ which has a number of important implications for collider phenomenology. First, the lightest standard model superpartner is now the next lightest supersymmetric particle (NLSP) and eventually decays into its standard model partner and the gravitino. The NLSP may then be charged or colored, as astrophysical and other constraints on such particles are thereby evaded. Second, the NLSP may be stable or unstable in collider experiments, depending on F_{DSB} . If F_{DSB} is high enough, decays to the gravitino is suppressed, and the NLSP decays outside the detector.

The possible collider phenomena in gauge-mediated models are largely determined by the character of the NLSP. Typically, in these models the NLSP is either the lightest neutralino or the stau mass eigenstate $\tilde{\tau}_1$.² As this particle may be either long- or short-lived,³ there are four broad possibilities. If the NLSP is a long-lived neutralino, the SUSY signatures are the

¹We assume that there are no other exotic light particles.

²In the latter case, the role of the NLSP may be shared by the sleptons \tilde{e}_R and $\tilde{\mu}_R$ if they are sufficiently degenerate with $\tilde{\tau}_1$.

³Throughout this paper, “long-lived” and “short-lived” refer to particles that typically decay outside and inside collider experiments, respectively.

conventional \cancel{E}_T signals and are identical to those present in gravity-mediated models with R -parity conservation. If the NLSP is a short-lived neutralino, superparticle production typically results in hard photons, a signal that has also been studied in great detail [3,4]. On the other hand, the NLSP could be the stau. In the case of a short-lived stau NLSP, there are a number of interesting new signatures, which have been studied in Refs. [5,6].

Here, we explore the remaining possible scenario, in which the NLSP is a long-lived stau. This scenario is in fact realized in large portions of the parameter space: as we will discuss in Sec. II, the stau is often the NLSP in models with non-minimal messenger sectors, and it is stable for $F_{\text{DSB}}^{1/2} \gtrsim 10^7$ GeV, as is also the case in many models, including, for example, the gauge mediation models of Ref. [2]. In this scenario, the familiar \cancel{E}_T and hard photon signals are absent. However, SUSY may manifest itself at colliders through a number of spectacular new phenomena. For example, staus, as massive charged particles, may be slow and appear as highly ionizing tracks [4,6,7]. If, on the other hand, the staus are quite relativistic, they cannot be distinguished from muons, and we may have excesses of dimuon or multi-lepton events as a result of superparticle production.

In this paper, we present a detailed discussion of the prospects for SUSY discovery in this scenario, and estimate the discovery reach for a variety of signatures. At present, the most stringent bound on these scenarios comes from searches for stable charged particles at LEP [8]. Such searches, using combined data from runs with center of mass energies up to $\sqrt{s} = 172$ GeV, yield the limit $m_{\tilde{\tau}_R} > 75$ GeV [9], where no degeneracy between generations is assumed. In this study, we begin by considering possible probes from Tevatron Run I data with $\sqrt{s} = 1.8$ TeV and an integrated luminosity of $L = 110$ pb $^{-1}$. Working within a specific, well-motivated model, we find that this currently available data probes regions of parameter space beyond the current LEP bound and even beyond the final LEP II kinematic limit. We then consider possible improvements at Tevatron Run II and the possible TeV33 upgrade. As a number of signals are essentially background-free, the prospects for improvement are especially bright. For $\sqrt{s} = 2$ TeV, and integrated luminosities of $L = 2, 10,$ and 30 fb $^{-1}$, we find that SUSY may be discovered for right-handed slepton masses of 110, 180, and 230 GeV and Wino masses of 310, 370, and 420 GeV, respectively. While exact discovery reaches must await detailed experimental analyses beyond the scope of this study, these results indicate that the prospects for such searches are promising, as future Tevatron runs will extend current search boundaries far into ranges typically expected for superpartner masses.

The organization of this paper is as follows. In Sec. II, we briefly review the framework of gauge-mediated supersymmetric models. We describe a particular, well-motivated model that displays many of the generic features of gauge mediation models, and which we will use throughout the rest of the paper. In the subsequent sections, we explore three new signatures for long-lived staus. For each, we first estimate the discovery reach in terms of physical slepton and gaugino masses. In Sec. III, we discuss the possibility of detecting the highly ionizing tracks of heavy charged NLSPs. In Sec. IV, we consider a possible excess of dimuon-like events due to the pair production of $\tilde{\tau}_1$. The dimuon excess is a relatively weak probe at the Tevatron; we discuss also its prospects at the LHC. We then discuss the multi-lepton signal in Sec. V. Finally, in Sec. VI we summarize all of these results by studying and comparing the discovery reaches of the various signals in the context of the model we consider and its fundamental parameter space. We present our conclusions in Sec. VII.

II. GAUGE-MEDIATED MODELS AND THE LONG-LIVED STAU NLSP

The probes discussed in the following sections are relevant for all models with charged particles that are stable within the detector, and thus they have wide applicability. Within the framework of SUSY, such particles are possible in a variety of settings. By far the most natural of these is in the context of gauge-mediated SUSY breaking models, where the NLSP may be charged and typically decays to the gravitino with macroscopic decay lengths.⁴

In the general framework of gauge mediation, any of the MSSM superpartners could in principle be the NLSP and stable in collider detectors. For concreteness, and to obtain quantitative results, we will specify a particular, well-motivated model. In this section, we briefly review this simple and calculable model, which we will use to determine the promise of various charged NLSP signatures. In doing so, we define our conventions and notation, and introduce the parameters that will play a central role in the following discussions. Further details of this model may be found in Refs. [4,10].

In the class of gauge mediation models we consider, there are three sectors: the dynamical SUSY breaking (DSB) sector, the messenger sector, and the MSSM sector. In the first, the F component of some chiral superfield condenses, generating a vacuum expectation value $F_{\text{DSB}} \neq 0$. F_{DSB} determines both the mass of the gravitino

$$m_{3/2} = \frac{F_{\text{DSB}}}{\sqrt{3}M_*}, \quad (1)$$

where $M_* = M_P/\sqrt{8\pi} \simeq 2.4 \times 10^{18}$ GeV is the reduced Planck mass, and the strength of its interactions through, for example,

$$\mathcal{L}_{\text{int}} = \frac{m_{\tilde{\tau}_R}^2}{F_{\text{DSB}}} \bar{\psi}_{\tau_R} \tilde{\tau}_R^* + \text{h.c.}, \quad (2)$$

where ψ is the longitudinal component of the gravitino, the Goldstino.

This dynamical SUSY breaking is mediated by two-loop effects to the messenger sector, which contains a singlet field S , and, we will assume, N_5 pairs of vector-like $\mathbf{5} + \bar{\mathbf{5}}$ representations of $\text{SU}(5)$, that is, N_5 vector-like representations of $\text{SU}(2)_L$ doublets, and N_5 vector-like representations of $\text{SU}(3)_C$ triplets, where $\text{SU}(2)_L$ and $\text{SU}(3)_C$ are the standard model gauge groups. (Such messenger field content preserves gauge coupling unification. Vector-like representations $\mathbf{10} + \bar{\mathbf{10}}$ of $\text{SU}(5)$ may also be present, and each is equivalent to 3 vector-like $\mathbf{5} + \bar{\mathbf{5}}$ representations for the following discussion.) The scalar and auxiliary components of the singlet field then get vacuum expectation values $\langle S \rangle$ and F_S , respectively, which generate SUSY breaking masses for the N_5 vector-like fields. We denote the scale of these masses, the messenger scale, by M .

Finally, once the messenger fields are integrated out at the scale M , soft SUSY breaking masses for the superparticles in the MSSM sector are generated. Letting

⁴Long-lived charged particles are also possible in gravity-mediated models if the decays of a charged superparticle, such as a chargino or charged slepton, are, for example, highly phase space suppressed, or are possible only through small R -parity violating couplings.

$$\Lambda \equiv \frac{F_S}{\langle S \rangle} , \quad (3)$$

and assuming $\Lambda \ll M$, we find that one-loop diagrams induce gaugino masses

$$M_i(M) = N_5 \Lambda c_i \frac{g_i^2(M)}{16\pi^2} , \quad (4)$$

where $i = 1, 2, 3$ for the $U(1)_Y$, $SU(2)_L$, and $SU(3)_C$ groups, $c_1 = \frac{5}{3}$, and $c_2 = c_3 = 1$. Two-loop diagrams induce the soft SUSY breaking sfermion squared masses

$$M_{\tilde{f}}^2(M) = 2N_5 \Lambda^2 \sum_{i=1}^3 C_i^f \left[\frac{g_i^2(M)}{16\pi^2} \right]^2 . \quad (5)$$

Here, $C_1^f = \frac{5}{3}Y^2$ with $Y = Q - T_3$ being the usual hypercharge, and $C_i^f = 0$ for gauge singlets, $\frac{3}{4}$ for $SU(2)_L$ doublets, and $\frac{4}{3}$ for $SU(3)_C$ triplets. Finally, trilinear scalar couplings (A terms) are also induced, but are highly suppressed, as they are generated at two-loops, but have dimensions of mass, not mass squared. They may be taken to vanish at the scale M .

Once the boundary conditions are given at the messenger scale M , SUSY breaking parameters at the electroweak scale can be obtained by renormalization group (RG) evolution.⁵ In particular, the Higgs mass squared can be driven negative by the large top Yukawa coupling constant, and hence break electroweak symmetry. In our analysis, we do not specify the mechanism by which the supersymmetric Higgs mass μ and SUSY breaking Higgs mixing mass m_3^2 are generated. Several attempts to explain the origin of these parameters may be found in the literature [2,11]. Here we regard them as free parameters. We then fix one combination of them by demanding the correct value of the Fermi constant using the tree-level Higgs potential. The remaining freedom may be specified by choosing $\tan \beta$, the ratio of the vacuum expectation values of the two neutral Higgs scalars, and $\text{sign}(\mu)$, where we follow the conventions of Ref. [12] in defining the sign of μ . Thus, the simple model we have defined has 4+1 free parameters:⁶

$$N_5, M, \Lambda, \tan \beta, \text{sign}(\mu) . \quad (6)$$

In this model with the radiative electroweak symmetry breaking condition, the mass eigenvalues and mixing parameters for all superparticles are determined once we fix these parameters.

⁵Throughout this study, we use one-loop RG equations unless otherwise noted.

⁶If all the couplings in the model are $\mathcal{O}(1)$, $\langle S \rangle$ and $F_S^{1/2}$ (and hence M and Λ) are of the same order. However, in general, there may be a hierarchy between them. For example, if the coupling constant for the S^3 term in the superpotential is small, and all other couplings in the superpotential are $\mathcal{O}(1)$, $\langle S \rangle$ is enhanced relative to F_S , resulting in $\Lambda \ll M$ [2]. Thus, in our analysis, we treat M and Λ as independent parameters.

While the determination of SUSY parameters at the electroweak scale requires detailed calculation, it is useful to discuss the qualitative features of the superparticle spectrum. In the model described above, usually $\mu > M_1, M_2$. Furthermore, as can be seen in Eq. (4), gaugino masses are proportional to the corresponding gauge coupling constants, and hence $M_1 < M_2$. As a result, $\chi_1^0 \approx \tilde{B}$ with mass $m_{\chi_1^0} \approx M_1$, and $\chi_2^0 \approx \tilde{W}^3$ and $\chi_1^\pm \approx \tilde{W}^\pm$ with masses $m_{\chi_2^0}, m_{\chi_1^\pm} \approx M_2$. In the scalar sector, sfermion masses are primarily proportional to the relevant gauge coupling constants. Therefore, squarks are typically much heavier than sleptons, and right-handed sleptons, which have only $U(1)_Y$ quantum numbers, are the lightest sfermions. The sleptons \tilde{e}_R and $\tilde{\mu}_R$ are almost degenerate, as Yukawa coupling effects are negligibly small. On the contrary, the tau Yukawa coupling may significantly lower the lighter stau mass through both RG evolution and left-right mixing. These effects are enhanced for large $\tan\beta$. The lightest scalar is thus the lighter stau $\tilde{\tau}_1$, which is predominantly $\tilde{\tau}_R$.

We are interested in the case where $m_{\tilde{\tau}_1} < m_{\chi_1^0}$ and $\tilde{\tau}_1$ is the NLSP. This relation is most strongly and obviously dependent on N_5 . As one can see in Eqs. (4) and (5), at the messenger scale, $M_i \propto N_5$, while $M_{\tilde{f}} \propto \sqrt{N_5}$; thus, large N_5 reduces $m_{\tilde{\tau}_1}/m_{\chi_1^0}$. There is also an important dependence on M , as RG evolution increases right-handed slepton masses relative to gaugino masses, and so large values of M increase $m_{\tilde{\tau}_1}/m_{\chi_1^0}$. As noted above, large values of $\tan\beta$ decrease $m_{\tilde{\tau}_1}$ and so reduce $m_{\tilde{\tau}_1}/m_{\chi_1^0}$. Finally, the ratio $m_{\tilde{\tau}_1}/m_{\chi_1^0}$ is independent of Λ and $\text{sign}(\mu)$ to the extent that the relation $m_{\tilde{\tau}_1}/m_{\chi_1^0} \approx M_{\tilde{\tau}_R}/M_1$ is valid, where $M_{\tilde{\tau}_R}$ and M_1 are the soft SUSY breaking parameters.

In Fig. 1, we show contours of $M_{\tilde{\tau}_R}(M_{\text{MSSM}}) = M_1(M_{\text{MSSM}})$ in the (M, N_5) plane for various $\tan\beta$ and $M_{\text{MSSM}} = 1$ TeV. (See also Ref. [13].) The shaded region is excluded by the requirement that the gauge coupling constants remain perturbative up to the GUT scale $M_{\text{GUT}} \simeq 2.0 \times 10^{16}$ GeV under two-loop RG evolution. Although $M_{\tilde{\tau}_R}$ and M_1 are only approximately the physical $\tilde{\tau}_1$ and χ_1^0 masses because of mixing effects and D -term contributions, this figure gives a qualitative picture of the parameter region where $\tilde{\tau}_1$ is the NLSP. For a minimal messenger sector with $N_5 = 1$, $\tilde{\tau}_1$ is not the NLSP (unless $\tan\beta$ is large [4,10]). However, for $N_5 \geq 2$, $\tilde{\tau}_1$ is the NLSP for a wide range of parameter space.

In Figs. 2 and 3, we give contour plots of the soft SUSY breaking parameter ratios $M_{\tilde{\tau}_R}/M_1$ and $M_{\tilde{l}_L}/M_2$, respectively, where these ratios are at the scale $M_{\text{MSSM}} = 1$ TeV. We fix $\tan\beta = 3$ for these plots. In the stau NLSP region allowed by perturbativity, $M_{\tilde{\tau}_R}/M_1 > 0.6$, and for a significant portion of this region, the NLSP and χ_1^0 are fairly degenerate. We see also that, in this region, it is almost always true that $M_{\tilde{l}_L} < M_2$. In addition, $M_{\tilde{l}_L}/M_2 > 0.7$, and for a significant portion of this region, the \tilde{l}_L and Wino states are also fairly degenerate. These observations will be of use in the following sections.

Given the interaction of Eq. (2), the $\tilde{\tau}_1$ decay width is

$$\Gamma_{\tilde{\tau}_1} = \frac{1}{16\pi} \frac{m_{\tilde{\tau}_1}^5}{F_{\text{DSB}}^2}, \quad (7)$$

and its decay length is

$$L \simeq 10 \text{ km} \times \langle\beta\gamma\rangle \left[\frac{F_{\text{DSB}}^{1/2}}{10^7 \text{ GeV}} \right]^4 \left[\frac{100 \text{ GeV}}{m_{\tilde{\tau}_1}} \right]^5, \quad (8)$$

where β is the $\tilde{\tau}_1$ velocity and $\gamma \equiv (1 - \beta^2)^{-1/2}$. For $F_{\text{DSB}}^{1/2} \gtrsim 10^7$ GeV, the NLSP may be considered stable in detectors, as the likelihood of an NLSP decaying within the detector is negligible for Tevatron luminosities and the typical allowed ranges of supersymmetric cross sections. Such values of $F_{\text{DSB}}^{1/2}$ are expected in many proposed models. For example, in typical messenger sector models, $F_{\text{DSB}}^{1/2}$ is likely to be larger than $\sim 10^7$ GeV if there is no fine-tuning; otherwise, the SUSY breaking scale in the MSSM sector is so low that slepton masses become lighter than the experimental limit [14]. There are also many other recently proposed models, including those based on direct gauge mediation, that give high SUSY breaking scales [13,15].⁷ In a wide variety of models, therefore, the stau decays outside the detector, and we will concentrate on this possibility for the rest of this study.

III. HIGHLY IONIZING TRACKS

Long-lived staus are charged, weakly interacting, penetrating particles, and so appear in the tracking and muon chambers of collider detectors with little associated energy deposition in calorimeters. They therefore look like muons. However, since long-lived staus must have mass above 75 GeV [9], their velocity is typically not large if produced at the Tevatron. Moderately relativistic charged particles lose energy in matter primarily through ionization. The rate of energy loss $-dE/dx$ is determined largely by the particle's velocity β , grows rapidly with decreasing β for low β [17], and may be measured in tracking chambers. As a result, the cross section of slow staus may be significant, and highly ionizing tracks may be a spectacular signal of such particles.

If the stau is the NLSP, all superparticles eventually decay to staus, and so all superpartner production processes may result in highly ionizing tracks. However, in typical gauge-mediated scenarios, superparticle production at the Tevatron is dominated by only a few processes. First, squarks, Higgsinos, and heavy Higgs bosons (which may decay to superparticles) are too heavy to be produced in significant numbers. Second, left-handed sleptons, though typically much lighter than these particles, are still significantly heavier than right-handed sleptons, and so, in terms of overall rate, the Drell-Yan production of left-handed sleptons is negligible relative to that for right-handed sleptons. The dominant processes are therefore right-handed slepton production and gaugino production. In the following subsections, we discuss these two processes and their potential for SUSY discovery in turn.

A. Slepton Production

At the Tevatron, direct right-handed slepton production takes place through the Drell-Yan processes

$$p\bar{p} \rightarrow \gamma^*, Z^* \rightarrow \tilde{\tau}_1 \tilde{\tau}_1^*, \tilde{e}_R \tilde{e}_R^*, \tilde{\mu}_R \tilde{\mu}_R^* . \quad (9)$$

⁷Note, however, that in a class of models without messenger sectors [16], $F_{\text{DSB}}^{1/2}$ can be as small as 10^4 to 10^5 GeV, and the NLSP may decay inside the detector.

Cross sections for a single generation of right-handed slepton production as a function of slepton mass are given in Fig. 4 for $\sqrt{s} = 1.8$ TeV and $\sqrt{s} = 2$ TeV.⁸ Here and in the following, we use MRS R1 parton distribution functions [19] and the BASES phase space integration package [20]. The cross sections for the different generations are nearly identical for small $\tan\beta$, since then $\tilde{\tau}_1 \approx \tilde{\tau}_R$ and the three sleptons are highly degenerate. In the cases of \tilde{e}_R and $\tilde{\mu}_R$ pair production, the directly produced slepton may either be stable within the detector or may decay through virtual Binos via $\tilde{l}_R \rightarrow l_R \tau \tilde{\tau}_1$ if kinematically allowed [7].⁹ However, in all cases, the signal is a highly ionizing track from a long-lived charged slepton with no hadronic activity within some isolation cone.

Highly ionizing tracks may be faked by a real muon that overlaps with another particle track, which enhances the measured $-dE/dx$. The role of the muon may also be played by a hadron that punches through to the muon chambers. However, such backgrounds typically arise when the muon or hadron is part of a jet, and so are drastically reduced by requiring the highly ionizing particle to be isolated from significant hadronic activity. CDF has reported [21] such a search for highly ionizing tracks. They require the slow particle track to have $|\eta| \leq 0.6$ so that it is detected in the highly shielded central muon upgrade detector. It is also required to have $-dE/dx$ corresponding to $0.4 < \beta\gamma < 0.85$. The lower limit ensures that the stau reaches the central muon detector. The upper limit corresponds roughly to the requirement that the track be at least twice minimally ionizing. Such cuts are similar to those imposed in LEP analyses to eliminate background [8]. They are also expected to reduce the background at the Tevatron to negligible levels [21], and are appropriate for future Tevatron upgrades [22]. We will assume that after all of these cuts, the signal is essentially background-free.¹⁰

We may now estimate the number of slepton pair events resulting in highly ionizing tracks. In Fig. 5, we plot the cross section for $\tilde{\tau}_1$ pair production for $\sqrt{s} = 2$ TeV, where we have required at least one $\tilde{\tau}_1$ with $|\eta| \leq 0.6$ and $\beta\gamma < 0.4, 0.7, 0.85$, and ∞ . Results for $\sqrt{s} = 1.8$ TeV are similar, and we omit the corresponding figure. We find that the requirement $\beta\gamma > 0.4$ has little effect on the signal. The efficiencies for satisfying the upper bound criterion $\beta\gamma < 0.85$ are 25%, 44%, and 65% for $m_{\tilde{\tau}_1} = 100, 200$, and 300 GeV, respectively. While this degrades the signal substantially, slow stau cross sections on the order of 0.1 fb are still possible at slepton masses of 200 GeV.

Finally, we determine the discovery reach for long-lived charged sleptons. We sum over

⁸Next-to-leading order effects have been shown recently to enhance the tree-level cross sections by 35% to 40% [18], and so improve our discovery reaches slightly.

⁹For a rather narrow range of parameters with $m_{\tilde{\tau}_1} < m_{\chi_1^0} < m_{\tilde{l}_R}$, decays $\tilde{l}_R \rightarrow l_R \chi_1^0$ are also possible [6], but we will not consider this scenario here.

¹⁰Note that measurements of $\beta\gamma = |\vec{p}|/m$ from $-dE/dx$ and p_T from the tracking chambers constrain m . This may be used to further reduce background, as the signal is peaked at $m = m_{\tilde{\tau}_1}$, while the background is not localized in m .

three generations.¹¹ To crudely simulate the effects of geometric triggering efficiencies and track quality requirements, we have included an assumed experimental detection efficiency of 75%. With the assumption that the cuts described above reduce the background to negligible levels, we require, for a given luminosity, a cross section after including cuts and efficiencies corresponding to 5 or more events for discovery. The resulting reaches for representative Tevatron data samples are

$$\begin{aligned}
m_{\tilde{l}_R} &= 50 \text{ GeV} & (\sqrt{s} = 1.8 \text{ TeV}, L = 110 \text{ pb}^{-1}) \\
m_{\tilde{l}_R} &= 110 \text{ GeV} & (\sqrt{s} = 2 \text{ TeV}, L = 2 \text{ fb}^{-1}) \\
m_{\tilde{l}_R} &= 180 \text{ GeV} & (\sqrt{s} = 2 \text{ TeV}, L = 10 \text{ fb}^{-1}) \\
m_{\tilde{l}_R} &= 230 \text{ GeV} & (\sqrt{s} = 2 \text{ TeV}, L = 30 \text{ fb}^{-1}) .
\end{aligned} \tag{10}$$

We see that the discovery reach of 50 GeV for the currently available Run I data is not competitive with current LEP analyses. However, for future Tevatron runs, the discovery reach will be competitive with and eventually surpass the kinematic limit of LEP II.

B. Gaugino Production

Aside from right-handed slepton production, the other major SUSY production mechanisms at the Tevatron are¹²

$$p\bar{p} \rightarrow W^* \rightarrow \chi_1^\pm \chi_2^0 \quad \text{and} \quad p\bar{p} \rightarrow \gamma^*, Z^* \rightarrow \chi_1^\pm \chi_1^\mp , \tag{11}$$

where the neutralinos and charginos are Wino-like. The other processes involving gauginos, $p\bar{p} \rightarrow W^* \rightarrow \chi_1^\pm \chi_1^0$ and $p\bar{p} \rightarrow Z^* \rightarrow \chi_{1,2}^0 \chi_{1,2}^0$, are suppressed by mixing angles in the gaugino limit, and we have checked that, throughout parameter space, these are not significant relative to those of Eq. (11). The cross sections for the processes of Eq. (11) are given in Fig. 6 for both $\sqrt{s} = 1.8 \text{ TeV}$ and 2 TeV , where here and in the rest of this subsection, we neglect neutralino and chargino mixings and take them to be pure Wino eigenstates. For equivalent gaugino and slepton masses, the gaugino cross sections are much larger, as they are not suppressed by the β^3 behavior of scalar production.

As in Sec. III A, we would like to plot cross sections for events with slow staus. The decays of gauginos are significantly more complicated than those of right-handed sleptons. Of course, the branching ratios and kinematic distributions of the cascade decays are completely determined once the fundamental model parameters are fixed. However, for the present

¹¹In the case where sleptons \tilde{e}_R and $\tilde{\mu}_R$ decay via $\tilde{l}_R \rightarrow l_R \tau \tilde{\tau}_1$, typically $\Delta m \equiv m_{\tilde{l}_R} - m_{\tilde{\tau}_1} \ll m_{\tilde{l}_R}, m_{\tilde{\tau}_1}$, and the $\tilde{\tau}_1$ is produced nearly at rest in the \tilde{l}_R rest frame. In the lab frame, the $\tilde{\tau}_1$ and \tilde{l}_R velocities are therefore similar, and so once sleptons \tilde{e}_R or $\tilde{\mu}_R$ are produced with low velocity, they result in a highly ionizing track, irrespective of subsequent decays.

¹²Contributions to gaugino production from t -channel squark diagrams are highly suppressed by large squark masses in the gauge mediation framework and are omitted in our analysis.

purposes, as we will show, the cascade decays are determined to a large extent by two rather more meaningful parameters, namely, the physical Wino and \tilde{l}_R masses. In this section, we therefore prefer to highlight this dependence by adopting a conservative simplifying assumption. (The implications of these results for the fundamental parameter space will be discussed in Sec. VI.)

From Fig. 3, we see that for almost all parameters in the long-lived stau scenario, and for all parameters when $N_5 \geq 3$, $m_{\tilde{l}_L} < m_{\chi_2^0}, m_{\chi_1^\pm}$. Winos therefore decay primarily to left-handed sleptons, as the other possible two-body decays to $W\chi_1^0$, $Z\chi_1^0$, and the “spoiler mode” $h^0\chi_1^0$ are all suppressed by mixing angles in the gaugino region. The neutral Wino decay modes are then

$$\begin{aligned}\chi_2^0 &\rightarrow \tilde{l}_L \tilde{l}'_L \rightarrow \tilde{l}_L l'_L \chi_1^0 \rightarrow \tilde{l}_L l'_L \tilde{l}_R \tilde{l}_R, \\ \chi_2^0 &\rightarrow \tilde{\nu}'_L \tilde{\nu}' \rightarrow \tilde{\nu}'_L \nu' \chi_1^0 \rightarrow \tilde{\nu}'_L \nu' \tilde{l}_R \tilde{l}_R,\end{aligned}\tag{12}$$

and the charged Wino decay modes are

$$\begin{aligned}\chi_1^+ &\rightarrow \tilde{l}_L \tilde{\nu}' \rightarrow \tilde{l}_L \nu' \chi_1^0 \rightarrow \tilde{l}_L \nu' \tilde{l}_R \tilde{l}_R, \\ \chi_1^+ &\rightarrow \nu' \tilde{l}_L^* \rightarrow \nu' \tilde{l}_L \chi_1^0 \rightarrow \nu' \tilde{l}_L \tilde{l}_R \tilde{l}_R,\end{aligned}\tag{13}$$

where we have omitted states related by charge conjugation. From Figs. 2 and 3, we see also that the $\tilde{l}_L\text{--}\chi_2^0$ and $\tilde{l}_R\text{--}\chi_1^0$ mass splittings are never more than $\sim 20\%$ to 30% and are smaller than this in much of the parameter space allowed by perturbativity. In the limit that these states are highly degenerate, there are only two energetic final state particles in the Wino rest frame for any of the possible decays: the lepton from \tilde{l}'_L or $\tilde{\nu}'_L$ decay, and the final state \tilde{l}_R . We therefore make the following simplification: in the rest frame of the parent gaugino, we assume that the only energetic particles are one lepton and the final \tilde{l}_R . The \tilde{l}_R velocity in this rest frame is then fixed by

$$\beta\gamma|_{\text{rest}} = \frac{M_2^2 - m_{\tilde{l}_R}^2}{2M_2 m_{\tilde{l}_R}},\tag{14}$$

where β is the slow slepton’s velocity and $\gamma = (1 - \beta^2)^{-1/2}$. The cross section for slow \tilde{l}_R production is then completely determined by M_2 and $m_{\tilde{l}_R}$.

In Figs. 7–9, we show slow \tilde{l}_R production cross sections for three values of $m_{\tilde{l}_R}/M_2$ and $\sqrt{s} = 2$ TeV, where we sum over the three slepton generations and employ the simplifying assumption described above. (Again, results for $\sqrt{s} = 1.8$ TeV are fairly similar, and the corresponding figures are not presented.) To account for the roughly 2π coverage of the central muon upgrade detector, we have assumed an η cut efficiency of 50%. From these figures, we see that for fixed gaugino mass, the cross sections are maximized for large $m_{\tilde{l}_R}$, that is, small $\beta\gamma|_{\text{rest}}$. For $M_2 = 400$ GeV, for example, the $\beta\gamma < 0.85$ efficiency is 62%, 32%, and 7% for $m_{\tilde{l}_R}/M_2 = 0.5, 0.4$, and 0.3 , respectively. This can be understood as a consequence of the low velocity of the heavy Winos in the lab frame, which implies that the \tilde{l}_R velocity in the lab frame is mostly determined by its velocity in the Wino rest frame. Note that our simplifying assumption implies that we have taken the maximal possible value of $\beta\gamma|_{\text{rest}}$. In regions of the parameter space where \tilde{l}_L and χ_2^0 (and $m_{\tilde{l}_R}$ and $m_{\chi_1^0}$) are non-degenerate at the 20% to 30% level, additional leptons can have significant energies. This

reduces $\beta\gamma|_{\text{rest}}$, and therefore increases the slow particle cross sections. Our approximation is therefore conservative.

To determine the discovery reach for long-lived sleptons from gaugino production, we include a 75% experimental efficiency and require 5 or more events for discovery, as in Sec. III A. The resulting discovery reaches in M_2 for our representative set of luminosities are

$$\begin{aligned} M_2 &= 120 \text{ to } 150 \text{ GeV} & (\sqrt{s} = 1.8 \text{ TeV}, L = 110 \text{ pb}^{-1}) \\ M_2 &= 220 \text{ to } 280 \text{ GeV} & (\sqrt{s} = 2 \text{ TeV}, L = 2 \text{ fb}^{-1}) \\ M_2 &= 270 \text{ to } 340 \text{ GeV} & (\sqrt{s} = 2 \text{ TeV}, L = 10 \text{ fb}^{-1}) \\ M_2 &= 310 \text{ to } 390 \text{ GeV} & (\sqrt{s} = 2 \text{ TeV}, L = 30 \text{ fb}^{-1}), \end{aligned} \tag{15}$$

where the ranges are for $m_{\tilde{l}_R}/M_2 = 0.3$ to 0.5 . Because the signal is background-free, the discovery reaches grow rapidly with luminosity, and future Tevatron runs substantially extend our reach in SUSY parameter space.

IV. DIMUON-LIKE EVENTS

As discussed in the previous section, a long-lived charged slepton appears in detectors as a muon. Thus, even if the velocity of such a slepton is too high to be seen as a highly ionizing track, slepton production can lead to an excess of events with muons and an apparent violation of lepton universality. In this section, we discuss the simplest example of such an excess, namely, an apparent excess in the number of dimuon events from right-handed slepton pair production.

The Drell-Yan production of long-lived $\tilde{\tau}_1$ pairs will appear as an event with essentially no jet activity and two high energy muon-like tracks with no \cancel{p}_T . The production of right-handed sleptons of the first two generations may also lead to this signature. For \tilde{e}_R and $\tilde{\mu}_R$, there are three possibilities: (1) they may be stable within the detector; (2) they may decay via $\tilde{l}_R \rightarrow l_R \tau \tilde{\tau}_1$ to leptons that are so soft that they cannot be clearly identified in the detector; or (3) they may decay to the NLSP and detectable leptons. In the first two cases, which are applicable when $\tan\beta$ is small and \tilde{e}_R , $\tilde{\mu}_R$ and $\tilde{\tau}_1$ are nearly degenerate, the pair production of smuons and selectrons contributes to the dimuon event sample. We will assume this to be the case in this section. This assumption is conservative, in the sense that in the third scenario, \tilde{e}_R and $\tilde{\mu}_R$ pair production contributes to spectacular multi-lepton signals, which are virtually background-free. Such signals will be discussed in the following section.

The backgrounds to dimuon signals with little \cancel{p}_T have been studied in the context of searches at CDF for new neutral gauge bosons via their decays $Z' \rightarrow \mu^+\mu^-$ [23]. The dominant background is from genuine muon pair production $p\bar{p} \rightarrow \mu^+\mu^-$.¹³ Before cuts, the

¹³Of the remaining backgrounds, the largest is cosmic rays [23]. This cross section is estimated to be less than 1 fb for invariant dimuon masses above 200 GeV [23], and is negligible relative to the muon pair background if well-understood.

$m_{\tilde{\tau}_1}$	2 fb^{-1}	10 fb^{-1}	30 fb^{-1}	Optimal p_T^{cut}
80 GeV	1.6σ	3.7σ	6.4σ	100 GeV
100 GeV	1.0σ	2.3σ	4.0σ	120 GeV
120 GeV	0.7σ	1.4σ	2.6σ	140 GeV
140 GeV	0.4σ	1.0σ	1.7σ	160 GeV
160 GeV	0.3σ	0.6σ	1.1σ	180 GeV
180 GeV	0.2σ	0.4σ	0.7σ	200 GeV

TABLE I. Statistical significances of deviations in the ratio $\sigma(\mu^+\mu^-)/\sigma(e^+e^-)$ from contributions of long-lived charged slepton pair production to dimuon events for integrated luminosities $L = 2, 10$, and 30 fb^{-1} and $\sqrt{s} = 2 \text{ TeV}$ at the Tevatron. The signal from slepton pair production is summed over the three generations. The cut parameter p_T^{cut} is chosen to maximize the significance; the optimal values used are shown.

cross section for this process is several orders of magnitude larger than that for slepton pair production. However, the signal to background ratio may be improved by requiring both muon-like tracks to have p_T greater than some fixed p_T^{cut} . In Fig. 10, we plot the cross sections for right-handed slepton pair and muon pair production at the Tevatron with $\sqrt{s} = 2 \text{ TeV}$ as a function of p_T^{cut} . Following Ref. [23], we require that at least one muon satisfy $|\eta| \leq 0.6$, and the other have $|\eta| \leq 1.0$ so that its p_T may be well-measured in the central tracking chamber. As is evident in Fig. 10, the p_T cut is highly effective for $p_T^{\text{cut}} \gtrsim 100 \text{ GeV}$.

To estimate the discovery potential for a dimuon excess, we look for an apparent violation of lepton universality in the ratio $\sigma(\mu^+\mu^-)/\sigma(e^+e^-)$. By considering this ratio instead of the absolute $\mu^+\mu^-$ cross section, large systematic uncertainties from luminosity measurements and renormalization scale dependence in next-to-leading order calculations are removed. The statistical significance of deviations in this ratio, in units of standard deviation σ , is given by $S/\sqrt{2B}$, where S is the number of slepton pair events, B is the number of muon pair events, and we have neglected differences in e and μ acceptances and systematic errors in determining these acceptances. For a given slepton mass, we calculate the ratio $S/\sqrt{2B}$ as a function of p_T^{cut} , and optimize the choice of p_T^{cut} to maximize $S/\sqrt{2B}$. We assume an overall muon trigger efficiency of 75%, and sum over the three slepton generations for S . In Table I, we show the optimized value of $S/\sqrt{2B}$ and the optimal choice of p_T^{cut} for various values of $m_{\tilde{\tau}_1}$ and L . The optimal p_T^{cut} is typically $p_T^{\text{cut}} \sim m_{\tilde{\tau}_1}$.

The discovery reach for a 3σ excess in dimuon events is below 50 GeV for Run I, and for future Tevatron upgrades is

$$\begin{aligned}
m_{\tilde{l}_R} &= 70 \text{ GeV} & (\sqrt{s} = 2 \text{ TeV}, L = 2 \text{ fb}^{-1}) \\
m_{\tilde{l}_R} &= 90 \text{ GeV} & (\sqrt{s} = 2 \text{ TeV}, L = 10 \text{ fb}^{-1}) \\
m_{\tilde{l}_R} &= 110 \text{ GeV} & (\sqrt{s} = 2 \text{ TeV}, L = 30 \text{ fb}^{-1}) .
\end{aligned} \tag{16}$$

We see that this discovery mode is clearly less powerful than the previous signal discussed in Sec. III, and we will see that it is also weaker than that of the following section. In fact, for an integrated luminosity of $L = 2 \text{ fb}^{-1}$, it is not possible to achieve a 3σ excess,

$m_{\tilde{\tau}_1}$	10 fb ⁻¹	100 fb ⁻¹	600 fb ⁻¹	Optimal p_T^{cut}
100 GeV	8.1 σ	26 σ	63 σ	150 GeV
200 GeV	2.4 σ	7.7 σ	19 σ	250 GeV
300 GeV	1.1 σ	3.4 σ	8.3 σ	350 GeV
400 GeV	0.5 σ	1.7 σ	4.1 σ	450 GeV
500 GeV	0.3 σ	0.9 σ	2.3 σ	550 GeV
600 GeV	0.2 σ	0.5 σ	1.3 σ	650 GeV

TABLE II. Same as in Table I, but for integrated luminosities $L = 10, 100$, and 600 fb^{-1} and $\sqrt{s} = 14 \text{ TeV}$ at the LHC.

given current bounds from LEP. However, this mode may still be useful as a supplementary signal. For example, if highly ionizing tracks consistent with a certain charged particle mass are seen, the discovery of even a small but quantitatively consistent dimuon excess could be an interesting confirmation of the supersymmetric interpretation of these exotic signatures. Note also that it may be possible to improve the sensitivity of the dimuon channel by loosening the η cuts, otherwise improving acceptance, or by combining data from the two detectors.

Given the rather weak results for the Tevatron, we consider the possibility of observing a dimuon excess from $pp \rightarrow \tilde{l}_R \tilde{l}_R^*$ at the LHC with $\sqrt{s} = 14 \text{ TeV}$. We require $\eta \leq 2.2$ for both sleptons, corresponding approximately to the muon coverage of both LHC experiments [24], and, as above, assume a 75% experimental detection efficiency and sum over 3 generations. In Table II we present results for integrated luminosities of 10 fb^{-1} (one year, low luminosity), 100 fb^{-1} (one year, high luminosity), and 600 fb^{-1} (corresponding to multi-year runs and/or combined data sets from the two detectors). Not surprisingly, the results are much improved. For example, for $L = 100 \text{ fb}^{-1}$, a 3σ excess will be discovered for $m_{\tilde{l}_R} \lesssim 300 \text{ GeV}$. Of course, at the LHC, a number of other signals of gauge-mediated supersymmetry are likely to be evident, and even squark and gluino cross sections may be substantial.

V. MULTI-LEPTON SIGNALS

If stau NLSPs are misidentified as muons, supersymmetric particle production can lead to events that appear to have large numbers of leptons in the final state. Here we focus on events with 5 or more isolated leptons and very little hadronic activity. Assuming that the probability for jets and photons to fake leptons is well under control, the backgrounds to such events are small, and so even a few signal events may constitute a discovery signal. Such multi-lepton states may result from either right-handed slepton or gaugino production, and, as in Sec. III, we consider these in turn.

A. Slepton Production

For small $\tan\beta$, right-handed slepton pair production leads to dimuon events, as analyzed in Sec. IV. However, for large $\tan\beta$, the intergenerational splitting from the tau Yukawa coupling may be substantial, and selectrons and smuons may decay to NLSPs and sufficiently energetic leptons to be detected as multi-lepton events.

To understand what values of $\tan\beta$ are required for this scenario, let us consider the various contributions to the intergenerational mass difference. Left-right stau mixing gives an important contribution,

$$\Delta m_{\text{LR}} \simeq \frac{m_\tau^2 \mu^2 \tan^2 \beta}{2m_{\tilde{\tau}_R}(m_{\tilde{\tau}_L}^2 - m_{\tilde{\tau}_R}^2)} . \quad (17)$$

In addition, the splitting receives contributions from RG evolution. Roughly speaking, this effect is proportional to $\ln(M/M_{\text{MSSM}})$ and the beta function for $M_{\tilde{\tau}_R}^2$, and hence may be estimated as

$$\begin{aligned} \Delta m_{\text{RG}} &\sim \frac{1}{2m_{\tilde{\tau}_R}} \times \frac{1}{4\pi^2} y_\tau^2 \times \mathcal{O} \left[m_{\tilde{\tau}_L}^2 \ln(M/M_{\text{MSSM}}) \right] \\ &\sim \frac{1}{2\pi^2} \times \mathcal{O} \left[\frac{m_{\tilde{\tau}_L}^4}{v^2 \mu^2} \ln(M/M_{\text{MSSM}}) \right] \times \Delta m_{\text{LR}} , \end{aligned} \quad (18)$$

where y_τ is the τ Yukawa coupling constant, $v = 246$ GeV, and in the last line we have assumed large $\tan\beta$. Δm_{RG} may be sizeable compared to Δm_{LR} when $m_{\tilde{\tau}_L}$ is large relative to the electroweak scale. In any case, both contributions reduce $m_{\tilde{\tau}_1}$ and they are both enhanced when $\tan\beta$ is large. As a result, mass differences between $\tilde{\tau}_1$ and the other right-handed sleptons can become larger than 5 to 10 GeV when $\tan\beta \gtrsim 10$. In Fig. 11, we plot the mass splitting $\Delta m \equiv m_{\tilde{e}_R} - m_{\tilde{\tau}_1} \simeq m_{\tilde{\mu}_R} - m_{\tilde{\tau}_1}$ as a function of $m_{\tilde{\tau}_1}$ for fixed $N_5 = 3$, $M = 10^5$ GeV, $\mu > 0$, and various $\tan\beta$. If $\tan\beta$ is small, $\Delta m < m_\tau$, and all three right-handed sleptons are stable in the detector. However, for $\tan\beta \gtrsim 10$, mass splittings of 10 GeV or larger are possible, and \tilde{e}_R and $\tilde{\mu}_R$ may decay inside the detector to electrons and muons that are likely to be observable.

We now assume that $\tan\beta$ is large enough that the resulting leptons from \tilde{e}_R and $\tilde{\mu}_R$ decay are detected. Right-handed selectron and smuon pair production then leads to final states $(ee, \mu\mu)\tau\tau\tilde{\tau}_1\tilde{\tau}_1$. We take the signal to be events with 5 or more isolated leptons with no significant hadronic activity. Backgrounds to such signals are extremely small, and we therefore require a discovery signal of 5 events. To roughly incorporate the effects of detector acceptances and τ branching ratios, we assume an overall experimental efficiency of 50%. From Fig. 4, but for 2 generations, we find the following discovery reaches for slepton masses:

$$\begin{aligned} m_{\tilde{l}_R} &= 70 \text{ GeV} \quad (\sqrt{s} = 1.8 \text{ TeV}, L = 110 \text{ pb}^{-1}) \\ m_{\tilde{l}_R} &= 140 \text{ GeV} \quad (\sqrt{s} = 2 \text{ TeV}, L = 2 \text{ fb}^{-1}) \\ m_{\tilde{l}_R} &= 190 \text{ GeV} \quad (\sqrt{s} = 2 \text{ TeV}, L = 10 \text{ fb}^{-1}) \\ m_{\tilde{l}_R} &= 230 \text{ GeV} \quad (\sqrt{s} = 2 \text{ TeV}, L = 30 \text{ fb}^{-1}) . \end{aligned} \quad (19)$$

B. Gaugino Production

As discussed in Sec. III B, in the stau NLSP scenario, Wino-like charginos and neutralinos typically decay through left-handed sleptons, with cascade decays given in Eqs. (12) and (13). Assuming that right-handed sleptons appear in the detector as muons, the final state therefore contains many charged leptons and no jets. For scenarios with gauginos that are highly degenerate with sleptons, some of the real leptons in the final state may be too soft to detect. However, this applies only to points extremely close to the $m_{\tilde{\tau}_1} = M_1$ boundary of Fig. 1, and we will assume that this is not the case. Gaugino production then results in the spectacular signal of from 5 to 7 charged leptons.¹⁴

As in Sec. V A, we take the signal to be 5 or more isolated leptons with little hadronic activity. We demand 5 events for a discovery signal, and again include an overall experimental detector efficiency of 50%. For the 7 lepton events, this is likely to be a rather conservative estimate, as only 5 or more need be detected. We may then determine the discovery reach for multi-lepton signals in this scenario from Fig. 6. The discovery reaches for our representative data samples are

$$\begin{aligned} M_2 &= 190 \text{ GeV} & (\sqrt{s} &= 1.8 \text{ TeV}, L = 110 \text{ pb}^{-1}) \\ M_2 &= 310 \text{ GeV} & (\sqrt{s} &= 2 \text{ TeV}, L = 2 \text{ fb}^{-1}) \\ M_2 &= 370 \text{ GeV} & (\sqrt{s} &= 2 \text{ TeV}, L = 10 \text{ fb}^{-1}) \\ M_2 &= 410 \text{ GeV} & (\sqrt{s} &= 2 \text{ TeV}, L = 30 \text{ fb}^{-1}) . \end{aligned} \tag{20}$$

The multi-lepton signal from Wino production is thus one of the most sensitive probes, and probes chargino and neutralino masses far into the ranges typically expected for Wino masses.

VI. COMPARISON OF RESULTS

In the previous 3 sections, we have considered a variety of SUSY discovery signals in the long-lived stau NLSP scenario. They are:

- (A) Highly ionizing tracks from slepton pair production (Sec. III A).
- (B) Highly ionizing tracks from Wino pair production (Sec. III B).
- (C) An excess of dimuon events from slepton pair production (Sec. IV).
- (D) Multi-lepton signals from slepton pair production (Sec. V A).
- (E) Multi-lepton signals from Wino pair production (Sec. V B).

¹⁴We assume here that \tilde{e}_R and $\tilde{\mu}_R$ do not further decay through $\tilde{l}_R \rightarrow l_R \tau \tilde{\tau}_1$. If such decays result in detectable leptons, the signals are even more spectacular.

For each of these signals, we have obtained discovery reaches in terms of physical right-handed slepton and/or Wino masses by the analyses described above. We have found that the discovery reach for slepton masses from (A), (C), and (D) are numerically weaker than those for gaugino masses from (B) and (E). However, in typical gauge mediation scenarios, the Winos are predicted to be substantially heavier than the right-handed sleptons. It is therefore of interest to determine what the relative strengths of these probes are in terms of the fundamental parameter space of the gauge mediation model.

In Figs. 12–15, we summarize all of our previous results by presenting discovery reaches in the fundamental parameter space for various integrated luminosities. We display these reaches in the (M, Λ) plane, and fix the remaining three parameters $\tan\beta = 3$, $\mu > 0$, and N_5 . The number of messenger representations is $N_5 = 3$ for Figs. 12 and 14; in Figs. 13 and 15, we illustrate the N_5 dependence of these results by taking $N_5 = 4$. For each point in the plane, the complete superpartner spectrum is specified, and, in these figures, D -terms for scalar masses and all mixing effects are included in calculating physical masses and production cross sections. In each figure, we shade the area in which $m_{\tilde{\tau}_1} > m_{\chi_1^0}$; in the remaining region, the stau is the NLSP.

To guide the eye in relating the fundamental model parameters to more physical parameters, we plot dotted contours of constant $m_{\tilde{\tau}_1}$. Also, since M_i/g_i^2 is invariant under one-loop RG evolution and the weak scale coupling constants $g_i(M_{\text{MSSM}})$ are known, the weak scale gaugino masses $M_i(M_{\text{MSSM}})$ are proportional to Λ , independent of M . In particular, the $\text{SU}(2)_L$ gaugino mass is given by

$$M_2(M_{\text{MSSM}}) = N_5 \Lambda \frac{g_2^2(M_{\text{MSSM}})}{16\pi^2} . \quad (21)$$

We therefore also give vertical axis labels for $M_2(M_{\text{MSSM}})$ with $M_{\text{MSSM}} = 1$ TeV. This axis gives approximately the physical masses of the Wino-like chargino and neutralino.

For each point in parameter space with a stau NLSP, we determine the potential for SUSY discovery for each signal according to the analyses described in Secs. III–V. Contours for signals (A), (C), and (D) therefore roughly follow contours of constant right-handed slepton mass, and contours for signal (E) roughly follow contours of constant chargino and neutralino mass. For signal (B), the contours also roughly follow chargino and neutralino mass contours, but rise slightly relative to these contours as M increases: in this direction, $m_{\tilde{l}_R}$ increases, and the signal is strengthened, as discussed in Sec. III B.

We begin by presenting results in Figs. 12 and 13 for the present Tevatron data sample of $L = 110 \text{ pb}^{-1}$ at $\sqrt{s} = 1.8$ TeV. Several comments are in order. First, we have assumed $\tan\beta = 3$, and so slepton production does not result in multi-lepton events. Signal (D) is therefore not applicable. Second, signals (A) and (C) are too weak to appear in the plots. These signals are both from slepton production, and are essentially dependent on only the right-handed slepton mass. Given only the current Run I data, they are therefore weaker than the current LEP bound of $m_{\tilde{\tau}_R} > 75$ GeV, independent of model assumptions. For signal (B), the reaches plotted are conservative, as discussed in Sec. III B. Finally, signal (E), multi-lepton events from Wino production, requires that the leptons from $\tilde{W} \rightarrow \tilde{l}_L$ and $\tilde{B} \rightarrow \tilde{l}_R$ transitions be energetic enough to be detected. For $N_5 = 3$ and 4, this is always true for the former decay in the stau NLSP region. However, the latter decay may result in soft leptons, and the bound from signal (E) is therefore weakened for points very close to the boundary of the shaded region. We have not included this effect in the figures.

For the particular parameters we have chosen, a number of interesting conclusions may be drawn. Given the current Run I data, the slepton production signals (A) and (C) are superseded by the requirement that the parameters yield the stau NLSP scenario in the first place. Thus, for low $\tan\beta$, only the gaugino production signals (B) and (E) provide non-trivial probes of the parameter space. However, even given only the current Tevatron data sample, signals (B) and (E) do probe regions of parameter space not excluded by the current LEP bound $m_{\tilde{\tau}_R} > 75$ GeV [9]. For $N_5 = 3$, we see from Fig. 12 that signal (B) is sensitive to parameter regions beyond this bound, and signal (E) probes regions with $m_{\tilde{\tau}_1} \approx 110$ GeV, which are even beyond the ultimate kinematic reach of LEP II. For $N_5 = 4$, the ratio $m_{\tilde{\tau}_1}/M_2$ is reduced, and the strength of gaugino production mechanisms relative to slepton mechanisms is slightly weakened. However, as seen in Fig. 13, signal (B) is still competitive with the current LEP bound, and signal (E) will significantly extend the reach of LEP II for certain values of M .

In the context of the stau NLSP scenario, if no signals are found in analyses of the available Tevatron data, current bounds on Wino masses will be extended to roughly 200 GeV. In addition, in the framework of the particular model we have described, an indirect bound on $m_{\tilde{\tau}_1}$ may be set. For example, for $N_5 = 3$, we see from Fig. 12 that stau masses below ≈ 90 GeV would be excluded by the absence of signal (E). Of course, such indirect bounds on stau masses rely heavily on the specific model assumptions described in Sec. II.

In Figs. 14 and 15, we present results for the same model parameters, but for future Tevatron runs with $\sqrt{s} = 2$ TeV and $L = 2, 10$, and 30 fb $^{-1}$. Again, as we have assumed $\tan\beta = 3$, discovery reaches from (D) multi-lepton signatures of slepton pair production are inapplicable. Signal (C) is again weak relative to the others. For integrated luminosities of 2 fb $^{-1}$ or more, direct probes of slepton masses from signal (A) and indirect probes from signals (B) and (E) all exceed $m_{\tilde{\tau}_1} \sim 100$ GeV, and SUSY discovery in these modes is possible, even given potential LEP II bounds on the stau mass. For $L = 2$ fb $^{-1}$, the multi-lepton gaugino production signal (E) is dominant, and indirectly excludes stau masses below ~ 120 GeV. However, for increasing luminosity, the relative importance of the slow slepton signal (A) increases. For $L = 10$ fb $^{-1}$ and $L = 30$ fb $^{-1}$, signal (A) becomes the most sensitive probe, with sensitivity to regions of parameter space with Wino masses in excess of 400 to 600 GeV.

VII. CONCLUSIONS

Gauge-mediated supersymmetry breaking models provide an elegant solution to one of the most puzzling issues in supersymmetry, namely, the supersymmetric flavor problem. The phenomenology of these models is to a large extent dominated by the character of the NLSP. In the most popular gauge mediation scenarios, there are four options, as the NLSP may be either the neutralino or stau, and may be either stable or unstable in detectors. Three of these scenarios have received fairly extensive attention in the past. In this study, we have given for the first time a detailed treatment of prospects for SUSY discovery at the Tevatron in the fourth scenario, in which the NLSP is a long-lived stau. As discussed in Sec. II, this scenario is realized in a wide range of parameter space in models with messenger sectors with $N_5 \geq 2$.

In such scenarios, all superparticles decay ultimately to the lighter stau $\tilde{\tau}_1$, which appears in collider detectors as a (possibly slow) muon. We have analyzed the prospects for discovering SUSY by detecting highly ionizing tracks from slow $\tilde{\tau}_1$ production, an apparent excess in dimuon events from stau pairs, and the appearance of spectacular multi-lepton events from superpartner pair production followed by decays.

Of the signals considered, the dimuon excess is least promising, as it suffers from the large background of genuine $\mu^+\mu^-$ production. Its use appears to be limited to confirming the supersymmetric interpretation of other, more sensitive signals. Note, however, that a dimuon excess is only the simplest example of an apparent violation of lepton universality from long-lived $\tilde{\tau}_1$ production. Many other possibilities exist. If a statistically significant excess of μ over e events appears in any event sample, we strongly encourage the investigation of the long-lived charged slepton hypothesis, either by looking for highly ionizing slow tracks in this event sample, or by forming distributions of kinematic variables under the assumption that the muons are in fact sleptons of some given mass.

The remaining signals are sufficiently spectacular that they are essentially background-free after the cuts we have detailed in Secs. III and V. We have analyzed various data samples, beginning with Run I data with $\sqrt{s} = 1.8$ TeV and integrated luminosity $L = 110$ pb $^{-1}$. With this current data, we find that the sensitivity from slepton production is not competitive with the current bound on long-lived staus of $m_{\tilde{\tau}_R} \gtrsim 75$ GeV from combined LEP analyses. However, Winos with masses beyond the LEP kinematic limit may be produced in significant numbers at the Tevatron. Wino pair production therefore probes regions of parameter space beyond the current LEP bound, and even beyond the possible ultimate kinematic reach of LEP II. The analysis of currently available Tevatron data therefore provides interesting new probes of the gauge mediation parameter space.

Given the great interest in future Tevatron upgrades, we then considered what improvements may be expected from future Tevatron data. As the backgrounds to the signals we consider are extremely suppressed, we find that significant improvements may be expected. For future Tevatron runs with integrated luminosities of 2, 10, and 30 fb $^{-1}$, we estimate that SUSY may be discovered for right-handed slepton masses of 110, 180, and 230 GeV and Wino masses of 310, 370, and 420 GeV, respectively. These new and spectacular signals are therefore sensitive to much of the typically expected superpartner mass range and provide a promising avenue for SUSY searches at Tevatron runs in the near future.

ACKNOWLEDGMENTS

We are especially grateful to D. Stuart for many helpful conversations concerning experimental issues in detecting highly ionizing tracks. We also thank K. Agashe, B. Dutta, H. Frisch, M. Graesser, T. Han, and I. Hinchliffe for discussions, and the Aspen Center for Physics for hospitality during the inception of this work. This work was supported in part by the Director, Office of Energy Research, Office of High Energy and Nuclear Physics, Division of High Energy Physics of the U.S. Department of Energy under Contract DE-AC03-76SF00098, and in part by the National Science Foundation under grant PHY-95-14797.

REFERENCES

- [1] M. Dine, W. Fischler, and M. Srednicki, Nucl. Phys. **B189**, 575 (1981); S. Dimopoulos and S. Raby, Nucl. Phys. **B192**, 353 (1981); C. Nappi and B. Ovrut, Phys. Lett. B, **113**, 175 (1982); M. Dine and W. Fischler, Nucl. Phys. **B204**, 346 (1982); L. Alvarez-Gaume, M. Claudson and M. Wise, Nucl. Phys. **B207** 96 (1982).
- [2] M. Dine and A. E. Nelson, Phys. Rev. D **48**, 1277 (1993); M. Dine, A. E. Nelson, and Y. Shirman, Phys. Rev. D **51**, 1362 (1995); M. Dine, A. E. Nelson, Y. Nir, and Y. Shirman, Phys. Rev. D **53**, 2658 (1996).
- [3] D. R. Stump, M. Wiest, and C. P. Yuan, Phys. Rev. D **54**, 1936 (1996); S. Dimopoulos, M. Dine, S. Raby, and S. Thomas, Phys. Rev. Lett. **76**, 3494 (1996); S. Ambrosanio, G. L. Kane, G. D. Kribs, S. P. Martin, and S. Mrenna, Phys. Rev. Lett. **76**, 3498 (1996); S. Dimopoulos, S. Thomas, and J. D. Wells, Phys. Rev. D **54**, 3283 (1996); K. S. Babu, C. Kolda, and F. Wilczek, Phys. Rev. Lett. **77**, 3070 (1996); S. Ambrosanio, G. L. Kane, G. D. Kribs, S. P. Martin, and S. Mrenna, Phys. Rev. D **54**, 5395 (1996); *ibid.*, **55**, 1372 (1997); H. Baer, M. Brhlik, C.-h. Chen, and X. Tata, Phys. Rev. D **55**, 4463 (1997).
- [4] S. Dimopoulos, S. Thomas, and J. D. Wells, Nucl. Phys. **B488**, 39 (1997).
- [5] D. A. Dicus, B. Dutta, and S. Nandi, Phys. Rev. Lett. **78**, 3055 (1997); *ibid.*, Phys. Rev. D **56**, 5748 (1997); B. Dutta and S. Nandi, hep-ph/9709511; K. Cheung, D. A. Dicus, B. Dutta, and S. Nandi, hep-ph/9711216.
- [6] S. Ambrosanio, G. D. Kribs, and S. P. Martin, Phys. Rev. D **56**, 1761 (1997).
- [7] S. Ambrosanio, G. D. Kribs, and S. P. Martin, hep-ph/9710217.
- [8] The DELPHI Collaboration, P. Abreu *et al.*, Phys. Lett. B **396**, 315 (1997); The ALEPH Collaboration, R. Barate *et al.*, Phys. Lett. B **405**, 379 (1997); The L3 Collaboration, M. Acciarri *et al.*, CERN-PPE/97-75; The OPAL Collaboration, K. Ackerstaff *et al.*, OPAL PN-306 (1997).
- [9] Results presented at the EPS Conference, Jerusalem, 1997, P. Janot, “Search for New Particles”; LEP SUSY Working Group, “Preliminary results from the combination of LEP experiments,” F. Cerutti, M. Fanti, P. Giacomelli, P. Kluit, and U. Schwickerath, LEPSUSYWG/97-01 (<http://www.cern.ch/lepsusy/>).
- [10] J. A. Bagger, K. Matchev, D. M. Pierce, and R.-J. Zhang, Phys. Rev. D **55**, 3188 (1997).
- [11] G. Dvali, G. F. Giudice, and A. Pomarol, Nucl. Phys. **B478**, 31 (1996); M. Dine, Y. Nir, and Y. Shirman, Phys. Rev. D **55**, 1501 (1997); T. Yanagida, Phys. Lett. B **400**, 109 (1997); P. Ciafaloni and A. Pomarol, Phys. Lett. B **404**, 83 (1997); H. P. Nilles and N. Polonsky, Phys. Lett. B **412**, 69 (1997); M. Dine, talk presented at SUSY97, hep-ph/9707413; S. Dimopoulos, G. Dvali, and R. Rattazzi, hep-ph/9707537; A. de Gouvêa, A. Friedland, and H. Murayama, hep-ph/9711264.
- [12] H. E. Haber and G. L. Kane, Phys. Rep. **117**, 75 (1985).
- [13] S. Dimopoulos, G. Dvali, R. Rattazzi, and G. F. Giudice, hep-ph/9705307.
- [14] A. de Gouvêa, T. Moroi and H. Murayama, Phys. Rev. D **56**, 1281 (1997).
- [15] See, *e.g.*, E. Poppitz, Y. Shadmi, and S. P. Trivedi, Phys. Lett. B **388**, 561 (1996); E. Poppitz and S. P. Trivedi, Phys. Rev. D **55**, 5508 (1997); N. Arkani-Hamed, J. March-Russell, and H. Murayama, hep-ph/9701286; H. Murayama, Phys. Rev. Lett. **79**, 18 (1997); L. Randall, Nucl. Phys. **B495**, 37 (1997); C. Csaki, L. Randall, and W. Skiba, hep-ph/9707386; N. Haba, N. Maru, and T. Matsuoka, Nucl. Phys. **B497**, 31 (1997); *ibid.*, Phys. Rev. D **56**, 4207 (1997); Y. Shadmi, Phys. Lett. B **405**, 99 (1997);

- M. A. Luty, hep-ph/9706554; M. A. Luty and J. Terning, hep-ph/9709306; Y. Shirman, hep-ph/9709383.
- [16] K. I. Izawa, Y. Nomura, K. Tobe, T. Yanagida, Phys. Rev. D **56**, 2886 (1997); Y. Nomura and K. Tobe, hep-ph/9708377.
 - [17] Particle Data Group, R. M. Barnett *et al.*, Phys. Rev. D **54**, 1 (1996).
 - [18] H. Baer, B. W. Harris, and M. H. Reno, hep-ph/9712315.
 - [19] A. D. Martin, R. G. Roberts, and W. J. Stirling, Phys. Lett. B **387**, 419 (1996).
 - [20] S. Kawabata, Comp. Phys. Comm. **41**, 127 (1986).
 - [21] K. Hoffman, in *Proceedings of the International Europhysics Conference on High Energy Physics*, Jerusalem, Israel, August 19–26, 1997, FERMILAB-CONF-97/430-E.
 - [22] D. Stuart, private communication.
 - [23] CDF Collaboration, F. Abe *et al.*, Phys. Rev. Lett. **79**, 2192 (1997).
 - [24] CMS Collaboration, Technical Proposal, CERN/LHCC/94-38 (1994); ATLAS Collaboration, Technical Proposal, CERN/LHCC/94-43 (1994).

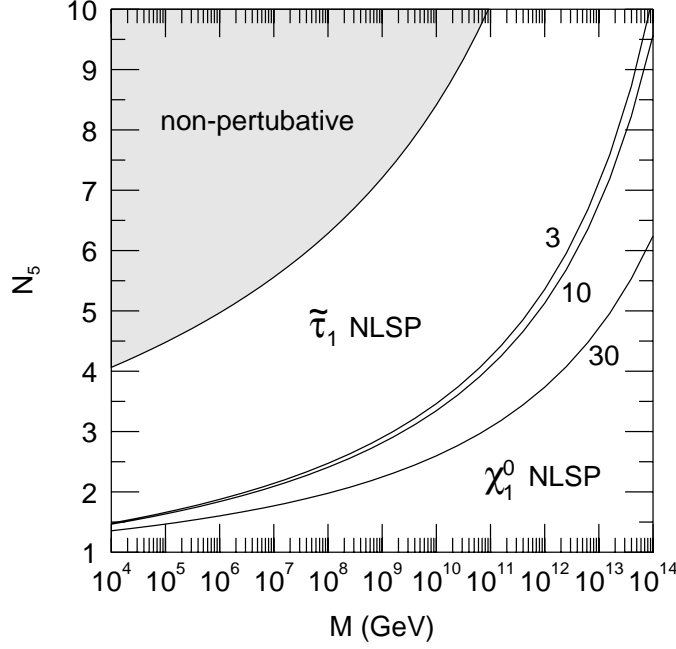


FIG. 1. Contours of $M_{\tilde{\tau}_R}(M_{\text{MSSM}}) = M_1(M_{\text{MSSM}})$ for $M_{\text{MSSM}} = 1$ TeV and $\tan \beta = 3, 10$, and 30 . In the region above the contours, $\tilde{\tau}_1$ is the NLSP; in the region below, χ_1^0 is the NLSP. In the shaded region, gauge coupling constants become non-perturbative below the GUT scale under two-loop RG evolution.

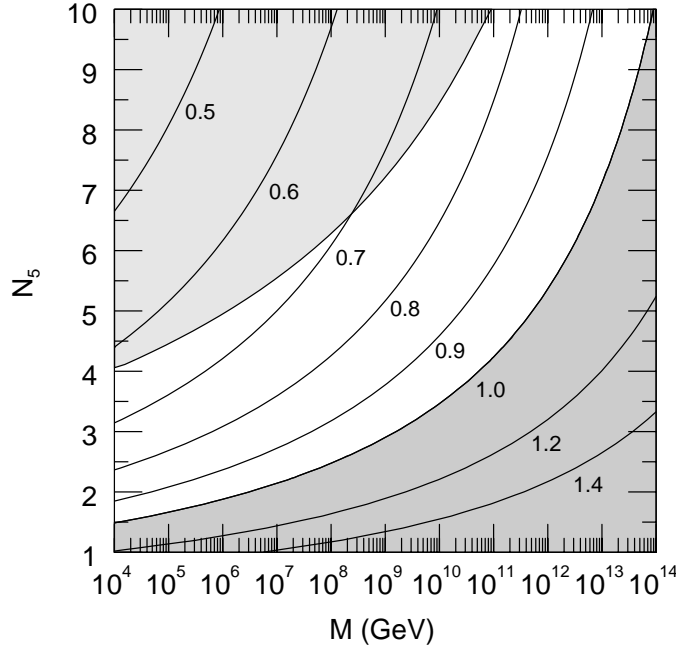


FIG. 2. Contours of the ratio of soft SUSY breaking parameters $M_{\tilde{\tau}_R}(M_{\text{MSSM}})/M_1(M_{\text{MSSM}})$ for $\tan \beta = 3$ and $M_{\text{MSSM}} = 1$ TeV. In the lower shaded region, $M_{\tilde{\tau}_R}(M_{\text{MSSM}}) > M_1(M_{\text{MSSM}})$. In the upper shaded region, gauge coupling constants become non-perturbative below the GUT scale.

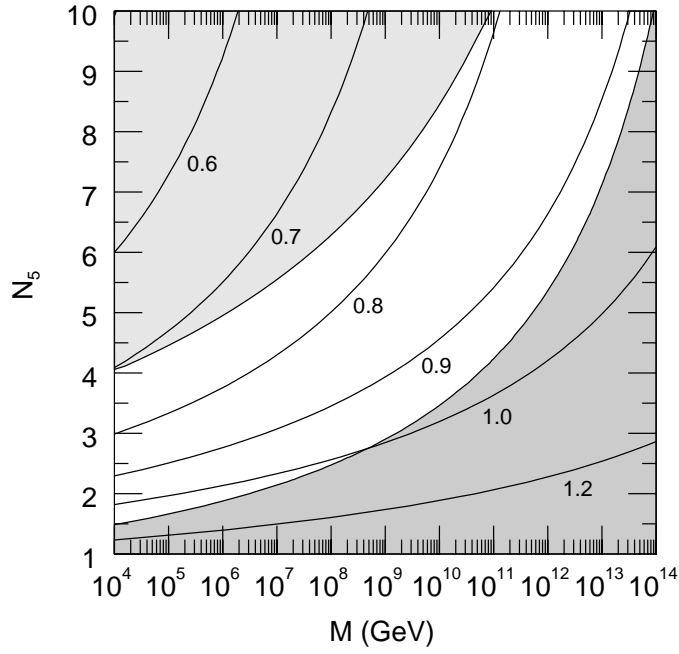


FIG. 3. Contours of the ratio of soft SUSY breaking parameters $M_{\tilde{t}_L}(M_{\text{MSSM}})/M_2(M_{\text{MSSM}})$ for $\tan \beta = 3$ and $M_{\text{MSSM}} = 1$ TeV. In the lower shaded region, $M_{\tilde{\tau}_R}(M_{\text{MSSM}}) > M_1(M_{\text{MSSM}})$. In the upper shaded region, gauge coupling constants become non-perturbative below the GUT scale.

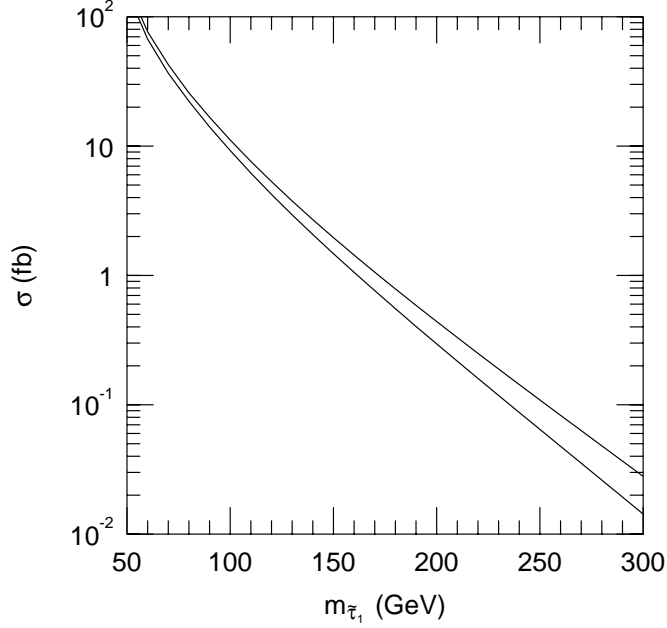


FIG. 4. Cross sections for $p\bar{p} \rightarrow \gamma^*, Z^* \rightarrow \tilde{\tau}_1 \tilde{\tau}_1^*$ for $\sqrt{s} = 1.8$ TeV (lower) and 2 TeV (upper), and $\tilde{\tau}_1 \approx \tilde{\tau}_R$.

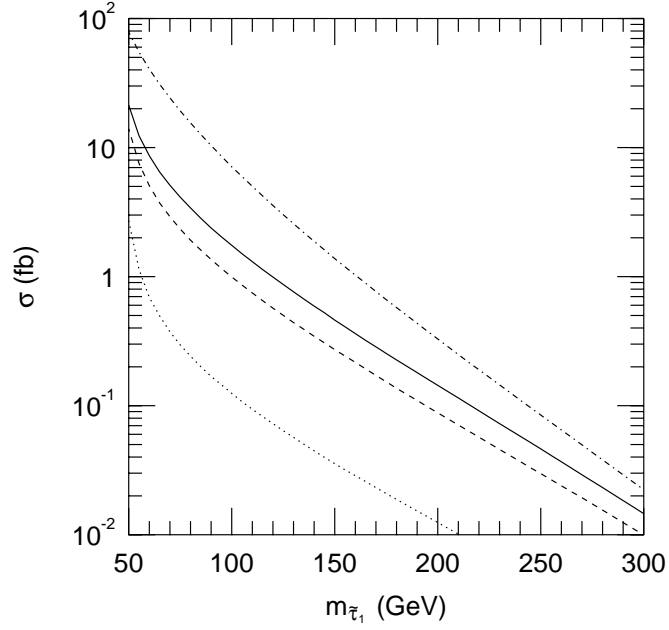


FIG. 5. Cross sections for the production of at least one slow $\tilde{\tau}_1$ from $p\bar{p} \rightarrow \gamma^*, Z^* \rightarrow \tilde{\tau}_1 \tilde{\tau}_1^*$ at $\sqrt{s} = 2$ TeV, where we have required $|\eta| \leq 0.6$ for the slow $\tilde{\tau}_1$. Contours correspond to $\beta\gamma \leq 0.4$ (dotted), 0.7 (dashed), 0.85 (solid), and ∞ (dot-dashed).

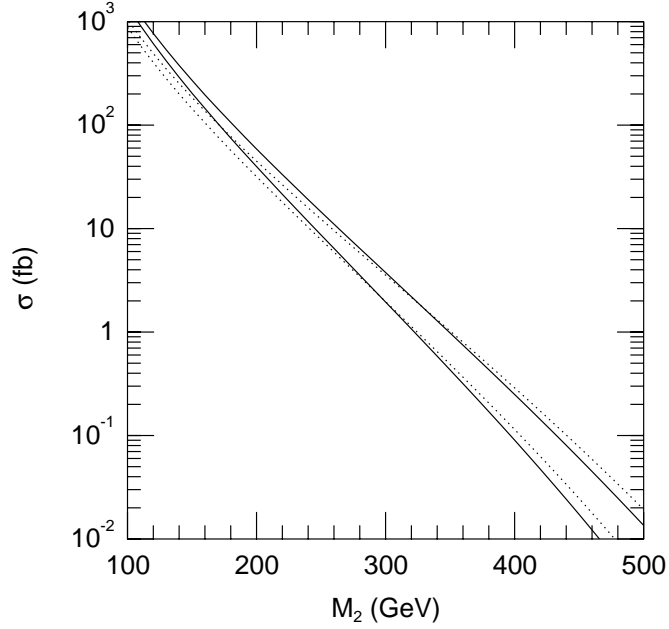


FIG. 6. Cross sections for $p\bar{p} \rightarrow W^* \rightarrow \chi_1^\pm \chi_2^0$ (solid) and $p\bar{p} \rightarrow \gamma^*, Z^* \rightarrow \chi_1^\pm \chi_1^\mp$ (dotted), for $\sqrt{s} = 1.8$ TeV (lower) and 2 TeV (upper). Chargino and neutralino mixing effects are neglected.

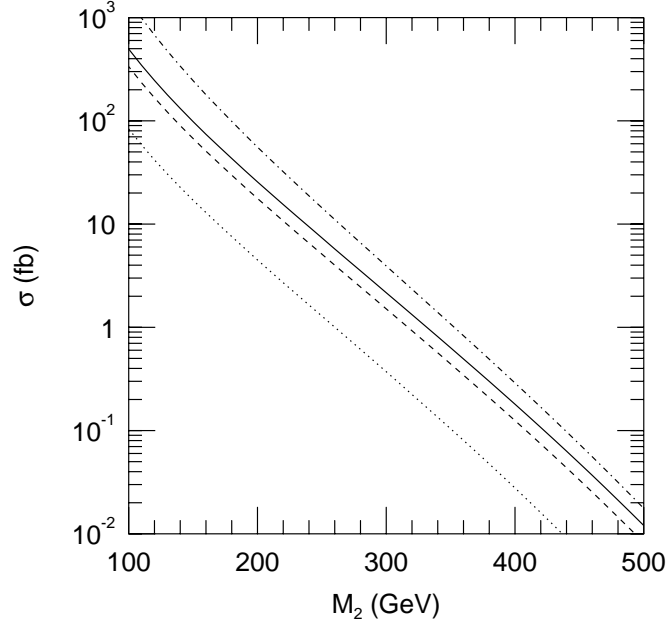


FIG. 7. Cross sections for slow \tilde{l}_R production from chargino and neutralino production with $m_{\tilde{l}_R}/M_2 = 0.5$, and summed over the three slepton generations. Contours correspond to $\beta\gamma \leq 0.4$ (dotted), 0.7 (dashed), 0.85 (solid), and ∞ (dot-dashed). An efficiency of 50% is included for the requirement that the slow slepton have $|\eta| \leq 0.6$.

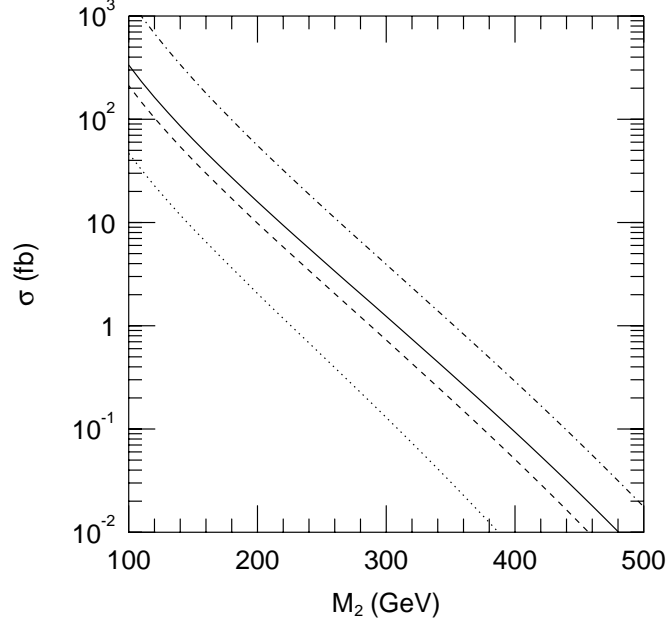


FIG. 8. Same as in Fig. 7, but for $m_{\tilde{l}_R}/M_2 = 0.4$.

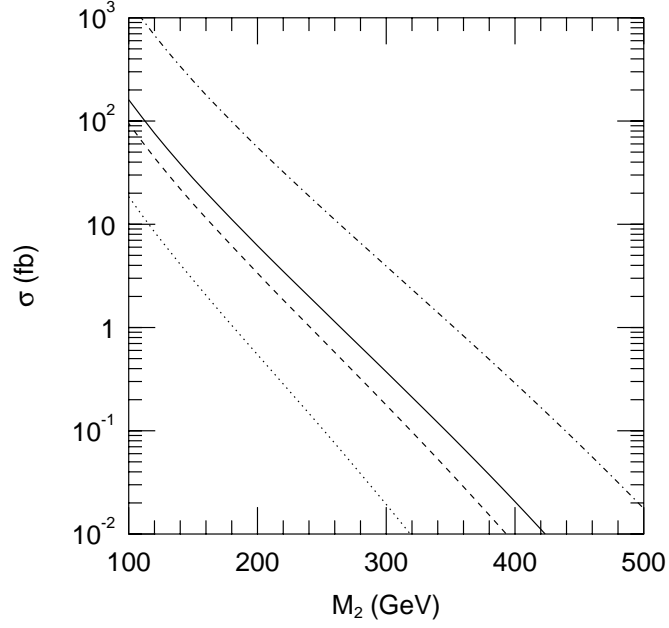


FIG. 9. Same as in Fig. 7, but for $m_{\tilde{l}_R}/M_2 = 0.3$.

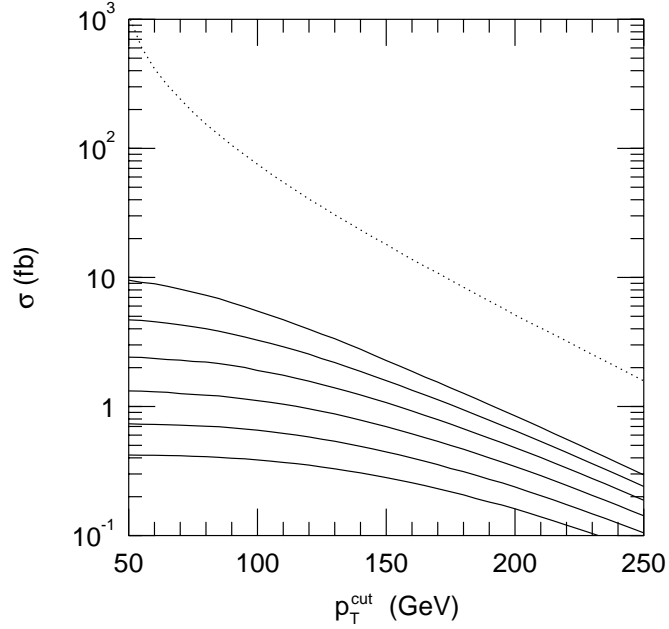


FIG. 10. The cross section for $\tilde{\tau}_1$ pair production at the Tevatron after requiring $p_T > p_T^{\text{cut}}$ for each stau, as a function of p_T^{cut} . We require one $\tilde{\tau}_1$ to have $|\eta| \leq 0.6$ and the other to have $|\eta| \leq 1.0$, and we take $\sqrt{s} = 2$ TeV and $m_{\tilde{\tau}_1} = 80, 100, 120, 140, 160$, and 180 GeV (solid lines from above). The cross section for the background $p\bar{p} \rightarrow \mu^+\mu^-$ is also shown (dotted).

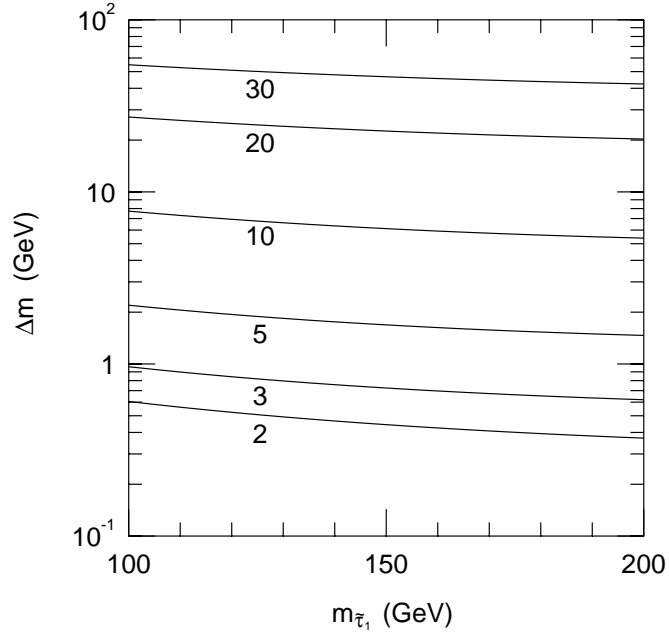


FIG. 11. The mass splitting $\Delta m = m_{\tilde{e}_R} - m_{\tilde{\tau}_1} \simeq m_{\tilde{\mu}_R} - m_{\tilde{\tau}_1}$ as a function of $m_{\tilde{\tau}_1}$ for fixed $N_5 = 3$, $M = 10^5$ GeV, $\mu > 0$, and the $\tan \beta$ values shown.

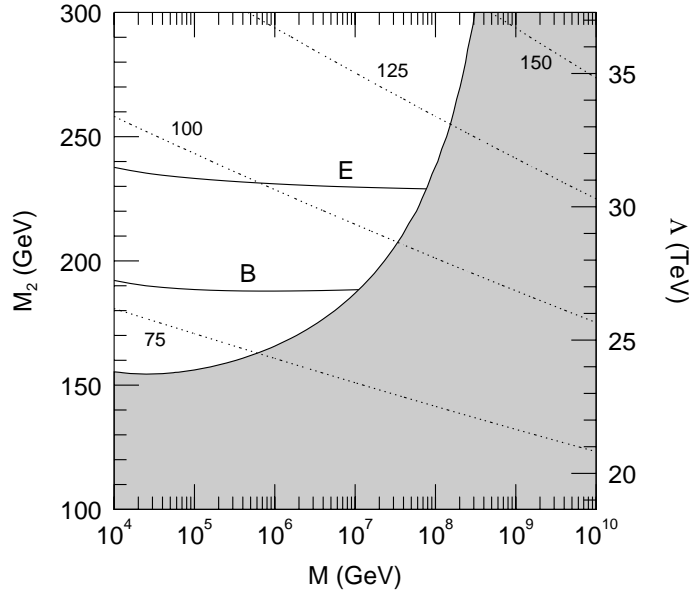


FIG. 12. Summary plot for $\sqrt{s} = 1.8$ TeV and $L = 110$ pb $^{-1}$ (Run I), and fixed $N_5 = 3$, $\tan \beta = 3$, and $\mu > 0$. Solid contours give the discovery reach for (B) highly ionizing tracks from gaugino production, and (E) multi-lepton signals from gaugino production. Contours of constant $m_{\tilde{\tau}_1}$ are given by the dotted curves. In the shaded region, $\tilde{\tau}_1$ is not the NLSP.

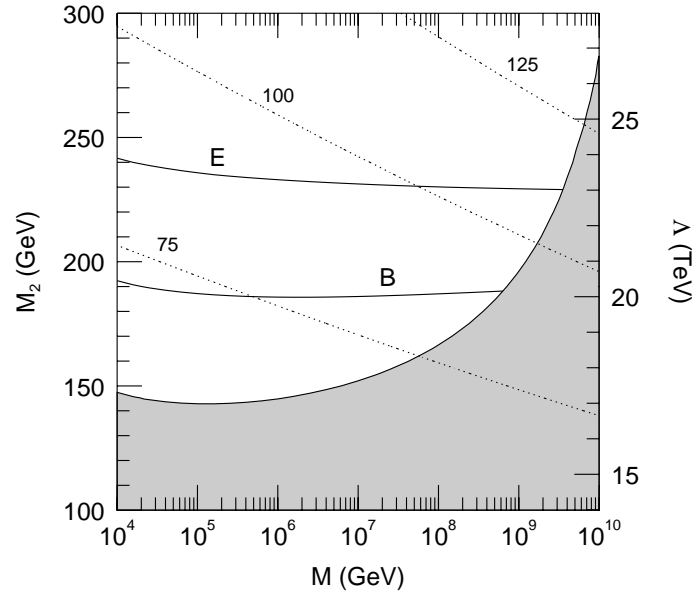


FIG. 13. Same as in Fig. 12, but for $N_5 = 4$.

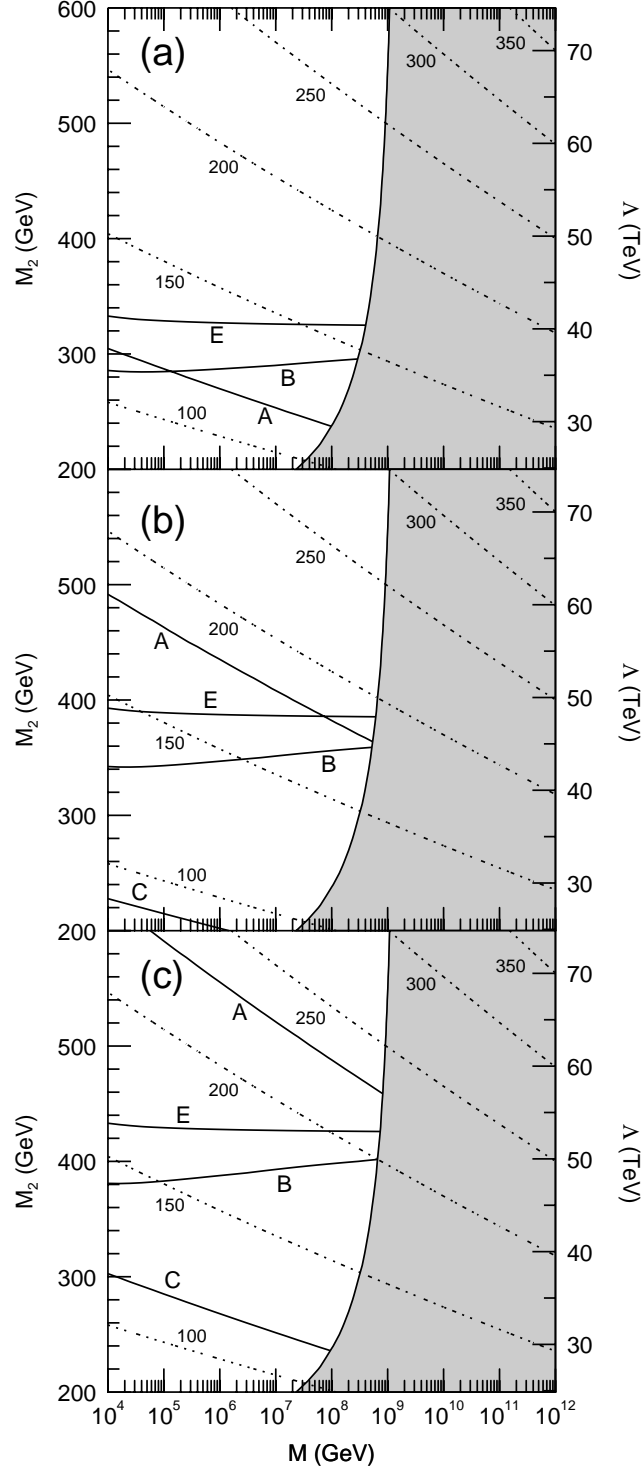


FIG. 14. Summary plot for $\sqrt{s} = 2$ TeV and integrated luminosity (a) 2 fb^{-1} , (b) 10 fb^{-1} , and (c) 30 fb^{-1} . We fix $N_5 = 3$, $\tan \beta = 3$, and $\mu > 0$. Solid contours give the discovery reach for (A) highly ionizing tracks from slepton production, (B) highly ionizing tracks from gaugino production, (C) a dimuon excess from slepton production, and (E) multi-lepton signals from gaugino production. Five events are required for (A), (B), and (E), and a 3σ excess is required for (C). Contours of constant $m_{\tilde{\tau}_1}$ are given by the dotted curves. In the shaded region, $\tilde{\tau}_1$ is not the NLSP.

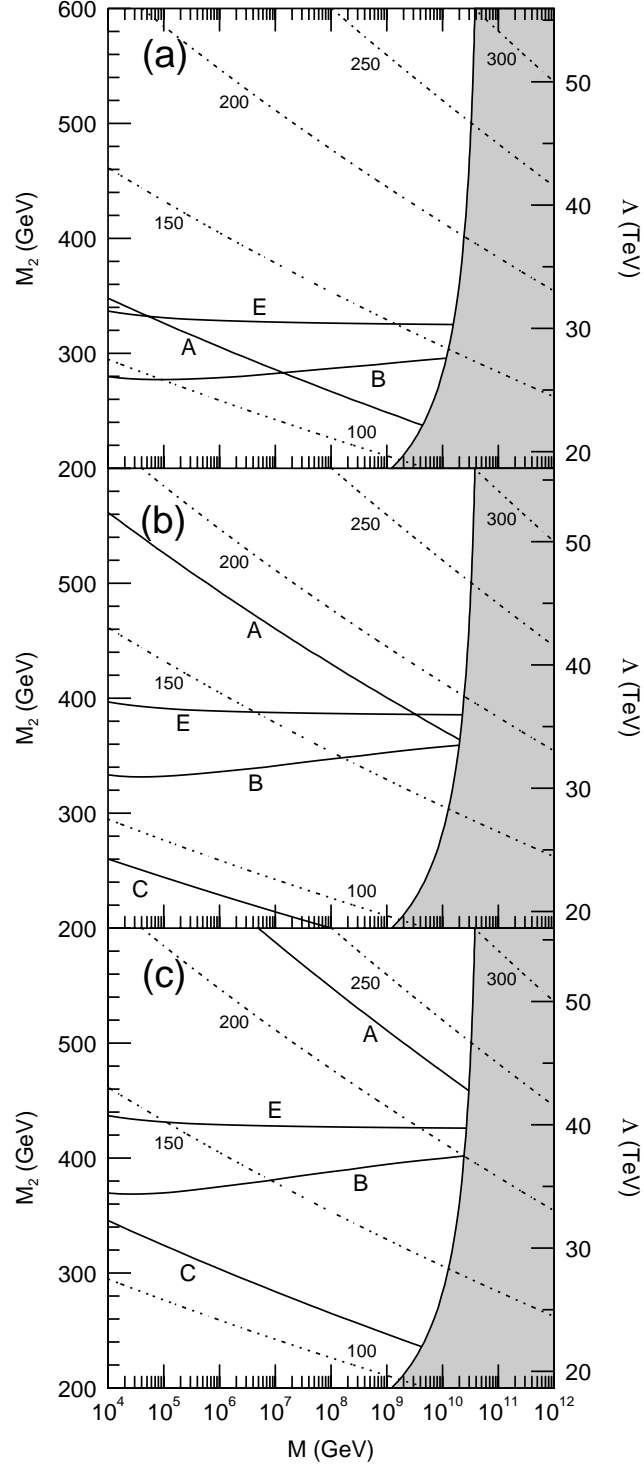


FIG. 15. Same as in Fig. 14, but for $N_5 = 4$.